Dopamine release from transplanted neural stem cells in Parkinsonian rat striatum in vivo

Xinjiang Kang[a,1], Huadong Xu[a,1], Sasa Teng[a,1], Xiaoyu Zhang[a], Zijun Deng[a], Li Zhou[a], Panli Zuo[a], Bing Liu[a], Bin Liu[a], Qihui Wu[a], Li Wang[a], Meiqin Hu[a], Haiqiang Dou[a], Wei Liu[a], Feipeng Zhu[a], Qing Li[a], Shu Guo[a], Jingli Gu[a], Qian Lei[a], Jing Lü[a], Yu Mu[a], Mu Jin[a], Shirong Wang[a], Wei Jiang[b], Kun Liu[c], Changhe Wang[a], Wenlin Li[d,2], Kang Zhang[b,e,f,2], and Zhuan Zhou[a,2]

[a]State Key Laboratory of Biomembrane and Membrane Biotechnology and Beijing Key Laboratory of Cardiometabolic Molecular Medicine, Institute of Molecular Medicine and McGovern Institute for Brain Research and Peking-Tsinghua Center for Life Sciences, Peking University, Beijing 100871, China; [b]Molecular Medicine Research Center, West China Hospital, Chengdu, Sichuan 610041, China; [c]Capital Sport University, Capital University of Physical Education and Sports, Beijing 100088, China; [d]Department of Cell Biology, Second Military Medical University, Shanghai 200092, China; [e]Institute of Genomic Medicine and Shiley Eye Center, University of California, San Diego, La Jolla, CA 92093; and [f]Veterans Administration Healthcare System, San Diego, CA 92161

Embryonic stem cell-based therapies exhibit great potential for the treatment of Parkinson's disease (PD) because they can significantly rescue PD-like behaviors. However, whether the transplanted cells themselves release dopamine in vivo remains elusive. We and others have recently induced human embryonic stem cells into primitive neural stem cells (pNSCs) that are self-renewable for massive/transplantable production and can efficiently differentiate into dopamine-like neurons (pNSC–DAn) in culture. Here, we showed that after the striatal transplantation of pNSC–DAn, (*i*) pNSC–DAn retained tyrosine hydroxylase expression and reduced PD-like asymmetric rotation; (*ii*) depolarization-evoked dopamine release and reuptake were significantly rescued in the striatum both in vitro (brain slices) and in vivo, as determined jointly by microdialysis-based HPLC and electrochemical carbon fiber electrodes; and (*iii*) the rescued dopamine was released directly from the grafted pNSC–DAn (and not from injured original cells). Thus, pNSC–DAn grafts release and reuptake dopamine in the striatum in vivo and alleviate PD symptoms in rats, providing proof-of-concept for human clinical translation.

dopamine | Parkinson's disease | striatum in vivo | neural stem cells | CFE

Parkinson's disease (PD) is a chronic progressive neurodegenerative disorder characterized by the specific loss of dopaminergic neurons in the substantia nigra pars compacta and their projecting axons, resulting in loss of dopamine (DA) release in the striatum (1). During the last two decades, cell-replacement therapy has proven, at least experimentally, to be a potential treatment for PD patients (2–7) and in animal models (8–15). The basic principle of cell therapy is to restore the DA release by transplanting new DA-like cells. Until recently, obtaining enough transplantable cells was a major bottleneck in the practicability of cell therapy for PD. One possible source is embryonic stem cells (ESCs), which can develop infinitely into self-renewable pluripotent cells with the potential to generate any type of cell, including DA neurons (DAns) (16, 17).

Recently, several groups including us have introduced rapid and efficient ways to generate primitive neural stem cells (pNSCs) from human ESCs using small-molecule inhibitors under chemically defined conditions (12, 18, 19). These cells are nonpolarized neuroepithelia and retain plasticity upon treatment with neuronal developmental morphogens. Importantly, pNSCs differentiate into DAns (pNSC–DAn) with high efficiency (~65%) after patterning by sonic hedgehog (SHH) and fibroblast growth factor 8 (FGF8) in vitro, providing an immediate and renewable source of DAns for PD treatment. Importantly, the striatal transplantation of human ESC-derived DA-like neurons, including pNSC–DAn, are able to relieve the motor defects in a PD rat model (11–13, 15, 19–23). Before attempting clinical translation of pNSC–DAn, however, there are two fundamental open questions. (*i*) Can pNSC–DAn functionally restore the striatal DA levels in vivo?

(*ii*) What cells release the restored DA, pNSC–DAn themselves or resident neurons/cells repaired by the transplants?

Regarding question 1, a recent study using nafion-coated carbon fiber electrodes (CFEs) reported that the amperometric current is rescued in vivo by ESC (pNSC–DAn-like) therapy (19). Both norepinephrine (NE) and serotonin are present in the striatum (24, 25). However, CFE amperometry/chronoamperometry alone cannot distinguish DA from other monoamines in vivo, such as NE and serotonin (Fig. S1) (see also refs. 26–28). Considering that the compounds released from grafted ESC-derived cells are unknown, the work of Kirkeby et al. was unable to determine whether DA or other monoamines are responsible for the restored amperometric signal. Thus, the key question of whether pNSC–DAn can rescue DA release needs to be reexamined for the identity of the restored amperometric signal in vivo.

Regarding question 2, many studies have proposed that DA is probably released from the grafted cells (8, 12, 13, 20), whereas others have proposed that the grafted stem cells might restore striatal DA levels by rescuing injured original cells (29, 30). Thus, whether the grafted cells are actually capable of synthesizing and

Significance

With a combination of HPLC and carbon fiber electrodes, we demonstrate that grafted neural stem cells directly release dopamine in the damaged striatum in vivo and partially rescue a Parkinson's disease (PD) model. (*i*) Primitive neural stem cell–dopamine-like neuron (pNSC–DAn) retained tyrosine hydroxylase expression and reduced the PD-like asymmetric rotation; (*ii*) depolarization-evoked dopamine release and reuptake were significantly rescued in striatum in vitro (brain slices) and in vivo, as determined jointly by microdialysis-based HPLC and electrochemical micro-carbon fiber electrodes; and (*iii*) the rescued dopamine was released directly from the grafted pNSC–DAn (not from the injured original cells). Thus, pNSC–DAn grafts release and reuptake dopamine in the striatum in vivo and alleviate PD symptoms in rats, providing proof-of-concept for human clinical translation.

releasing DA in vivo must be investigated to determine the future cellular targets (residual cells versus pNSC–DAn) of treatment.

To address these two mechanistic questions, advanced in vivo methods of DA identification and DA recording at high spatiotemporal resolution are required. Currently, microdialysis-based HPLC (HPLC) (31–33) and CFE amperometric recordings (34, 35) have been used independently by different laboratories to assess evoked DA release from the striatum in vivo. The major advantage of microdialysis-based HPLC is to identify the substances secreted in the cell-grafted striatum (33), but its spatiotemporal resolution is too low to distinguish the DA release site (residual cells or pNSC–DAn). In contrast, the major advantage of CFE-based amperometry is its very high temporal (ms) and spatial (μm) resolution, making it possible to distinguish the DA release site (residual cells or pNSC–DAn) in cultured cells, brain slices, and in vivo (34–39), but it is unable to distinguish between low-level endogenous oxidizable substances (DA versus serotonin and NE) in vivo.

In the present study, we developed a challenging experimental paradigm of combining the two in vivo methods, microdialysis-based HPLC and CFE amperometry, to identify the evoked substance as DA and its release site as pNSC–DAn in the striatum of PD rats.

Results

DA Release from Cultured pNSC–DAn. As described previously, we differentiated human ESCs into pNSCs using small-molecule inhibitors that inhibit glycogen synthase kinase 3 and the transforming growth factor beta (TGF-β) and Notch signaling pathways. These pNSCs resemble nonpolarized neuroepithelia and remain stably renewable in vitro. Importantly, they retain plasticity and can generate midbrain DA-like neurons or hindbrain motor neurons with high efficiency after being patterned with the appropriate morphogens (18) (see also refs. 12, 19). After treatment with SHH and FGF8, pNSCs consistently produced ~65% tyrosine hydroxylase (TH)-positive neurons, and most of the differentiated cells also expressed the mature neuron marker microtubule-associated protein 2 (MAP2) and the midbrain marker nuclear receptor related 1 protein (Nurr1) (Fig. 1A), indicating that the pNSCs had transformed into DA-like neurons (pNSC–DAn). Considering the potential application of pNSC–DAn in cell-replacement therapy, it was important to determine whether they were functional DA-releasing cells. HPLC analysis demonstrated the release of DA from pNSC–DAn in response to stimulation with 50 mM K$^+$ in Krebs–Ringer solution (Fig. 1 B and C). Consistently, 3,4-dihydroxyphenylacetic acid (DOPAC), a metabolite of DA, was also detected during the depolarizing stimulation (Fig. 1 B and C). To quantify the DA release from these cells, correlation curves between the concentrations of standard samples (DA and DOPAC) and their corresponding peak areas in HPLC were calculated. The calibration formulas of the analyte were as follows: y = 0.60x − 0.0012 (r^2 = 0.999) for DA, and y = 0.53x − 0.0022 (r^2 = 0.999) for DOPAC (y, peak area; x, analyte concentration in μM; Fig. S2D). The concentrations of DA and DOPAC from differentiated pNSC–DAn increased in the presence of 50 mM K$^+$ (Fig. 1C). In contrast, NE was not detected after stimulation with 50 mM K$^+$ (Fig. S3), excluding the possibility of NE release from these TH-positive pNSC–DAns.

Transplantation of pNSC–DAn Relieves the Asymmetric Rotation Defect in PD Rats. To determine whether the pNSC–DAns relieve Parkinsonian syndrome, we transplanted these cells into the ipsilateral striatum at week 4 after unilateral administration of 6-hydroxydopamine (6-OHDA) into the medial forebrain bundle (MFB). To identify the transplanted cells, these pNSCs were infected with lentivirus carrying GFP under the control of the EF-1α promoter, as previously reported (Fig. 2A) (18). Most of the GFP-labeled grafted cells survived and remained TH-positive 1 wk after transplantation (Fig. 2B). Importantly, the surviving cells still exhibited TH and MAP2 staining in the grafted area 16 wk after transplantation (Fig. 2C and Fig. S4). Further characterization
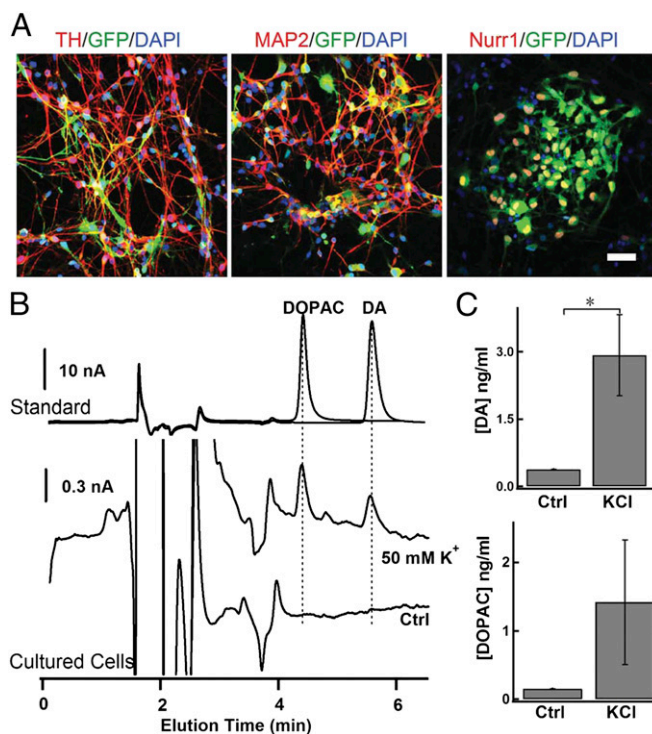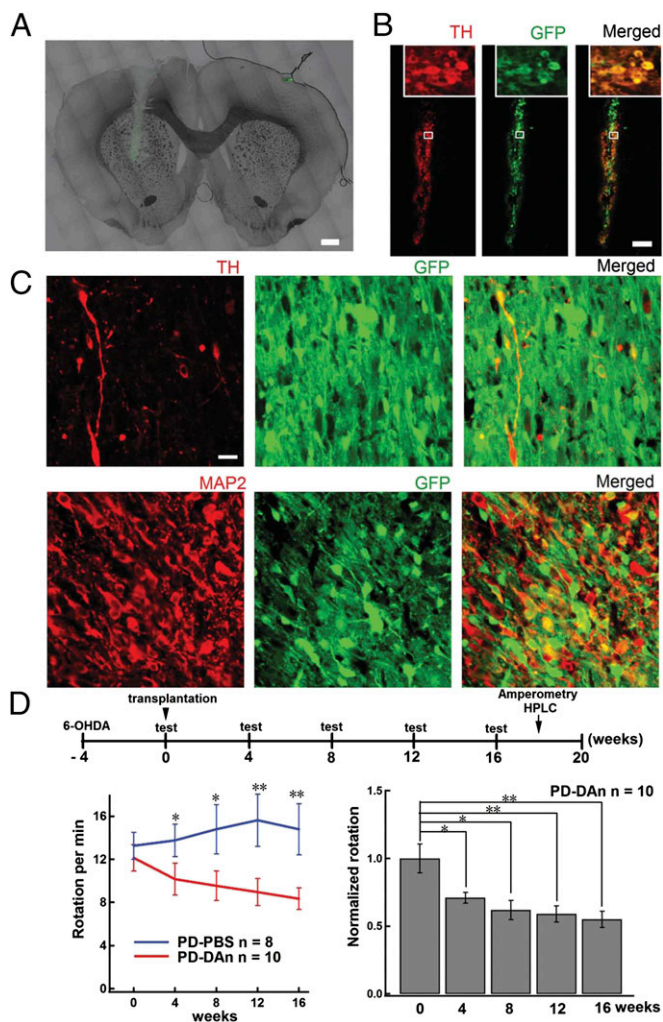

Fig. 1. Cultured pNSC-differentiated DA neurons (pNSC–DAn) are able to release DA. (A) Representative images of immunostaining for TH, MAP2, and Nurr1 in pNSC–DAn. (Scale bar, 50 μm.) (B) HPLC for DA and its derivative DOPAC in pNSC–DAn (differentiated for 2 mo) with or without 50-mM K$^+$ stimulation. (Top) HPLC chromatograms of standard samples of DOPAC (1 μM) and DA (1 μM). (Middle and Bottom) HPLC chromatograms of pNSC–DAn with 50-mM K$^+$-containing (Middle) or control Krebs–Ringer solution (Bottom). (C) Statistics of DA and DOPAC secreted from cultured pNSC–DAn with (high K$^+$, KCl) or without (Ctrl) 50-mM K$^+$ stimulation (Student t test; *P < 0.05).

also revealed the expression of DA D2 receptor, aldehyde dehydrogenase 1 (ALDH1A1), and vesicular monoamine transporter-2 (VMAT2) in grafted cells, indicating the persistence of mature DAns in vivo (Fig. S5). The apomorphine-induced asymmetric rotation was assessed every 4 wk from the day of transplantation until 16 wk (Fig. 2D). Note, compared with the PBS-injected PD rats (PD–PBS), animals with pNSC–DAn (PD–DAn) showed a significant and progressive reduction in contralateral rotations over time (Fig. 2D, Lower Left). Compared with that before transplantation, there was a gradual and significant recovery in rotation in PD–DAn rats during the 16 wk after transplantation (Fig. 2D, Lower Right).

Grafted Cells Restore Stimulus-Induced DA Overflow in PD Striatum in Vivo. The concentration of DA and its metabolites in PD–PBS, PD–DAn, and intact striatum were analyzed for evoked DA release in vivo by microdialysis-based HPLC, which provided unequivocal chemical verification of depolarization-dependent electrochemical signals including DA rather than NE and serotonin. In the intact striatum, the DA signal increased significantly with 70-mM K$^+$ stimulation, which was consistent with the stimulus dependence of DA secretion in the striatum (Fig. S2). Compared with that in the control side, DA and its metabolites DOPAC and homovanillic acid (HVA) decreased remarkably in the PD–PBS striatum (Fig. 3). The diminished DA signal in the PD striatum was partially rescued by the pNSC–DAn grafts (Fig. 3) (PD–DAn, 0.011 ± 0.004 μM; PD–PBS, 0.002 ± 0.0002 μM; P < 0.05). After pNSC–DAn transplantation, the DA level in the PD–DAn striatum recovered to ~6% of that in the intact side (Fig. 3). These results confirmed that the grafted pNSC–DAn relieved the rotation defect probably due to the increased DA level in the striatum.
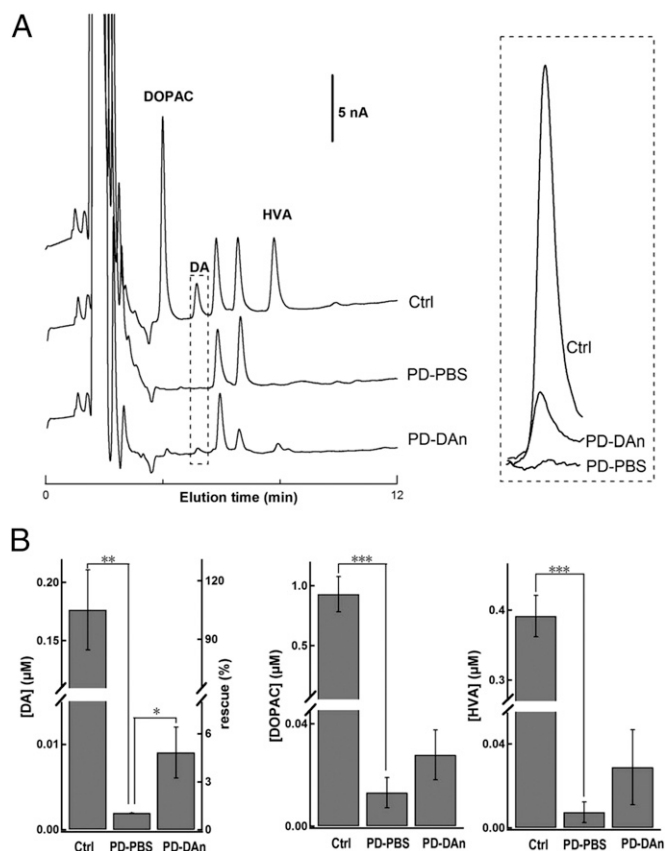
slices from the lesioned side of PD–PBS rats (Fig. 4 *B* and *D*) (intact control, 505.0 ± 61.6 pA; PD–PBS, 6.1 ± 1.1 pA; $P < 0.001$). However, the evoked DA overflow was partially restored in PD–DAn slices (Fig. 4 *B* and *D*) (6.1 ± 1.1 pA; PD–DAn, 26.1 ± 7.4 pA, $P < 0.01$), and occurred exclusively in the grafted regions (Fig. 4 *C* and *E*) (outside graft, 2.8 ± 0.8 pA; inside graft, 25.6 ± 6.3 pA; $P < 0.01$). The specificity of DA release in the GFP-positive area was consistent with the observation that the grafted pNSC–DAn remained TH-positive and that the TH-positive staining was mainly detected in GFP-positive cells and processes (Fig. 2 *A–C* and Fig. S4). Combined with the absence of TH staining in the striatum on the lesioned side (Fig. S7) and that the differentiated pNSCs secreted DA in vitro, these findings demonstrated that the increased DA signal in the striatum is due to direct release from the grafted pNSC–DAn.

Grafted Neurons Partially Rescue DA Release in PD Rats in Vivo. To further assess the potential therapeutic effect of grafted cells, we performed in vivo amperometric recordings in anesthetized PD–DAn rats. Electrical stimulation of the DA fibers in the MFB is commonly used to evoke DA release in the striatum in vivo (34). However, the original MFB and striatal DA terminals on the lesioned side in PD–DAn rats were damaged, so we designed a "stimulus secretion-coupling electrode" that delivered high K^+ locally to depolarize the original or grafted cells under the

Fig. 2. Grafted pNSC–DAns survive for at least 16 wk and reduce asymmetric rotation in the PD rat model. (*A*) Representative micrographs of pNSC–DAn grafts in the striatum. The transplantation track is visible. (Scale bar, 1 mm.) (*B*) Representative immunomicrograph showing that the GFP-labeled pNSC–DAn colocalized with TH staining (red) 1 wk after transplantation. (Scale bar, 100 μm.) (*C*) TH (*Upper* panels, red) and MAP2 (*Lower* panels, red) colocalized with GFP-labeled pNSC–DAn 16 wk after transplantation. (Scale bar, 20 μm.) (*D*) Apomorphine-induced asymmetric rotation in 6-OHDA–lesioned rats was relieved for 16 wk after transplantation with pNSC–DAn. (*Upper*) Schematic of the experimental procedure. (*Lower Left*) Apomorphine-induced rotation in PD–PBS and PD–DAn rats (Student *t* test; *$P < 0.05$, **$P < 0.01$). (*Lower Right*) Apomorphine-induced rotation in PD–DAn rats declined over time after transplantation (ANOVA; *$P < 0.05$, **$P < 0.01$).

Grafted Neurons Partially Rescue DA Release in Striatal Slices. DA and its metabolites are easily oxidizable and can be detected by both HPLC (32, 33), which can identify substances (Fig. S2), and CFE amperometry (34, 35, 37, 38, 40), which has extremely high spatial and temporal resolution. Because the evoked release of DA and its metabolites had been confirmed by HPLC (Fig. 3), we performed amperometric recordings in striatal slices to determine whether the increased DA level in the striatum was due to its release from grafted pNSC–DAn. Because the pNSCs expressed GFP, the grafted neurons and fibers were clearly visible under a fluorescence microscope (Fig. 4*A*, *Left*), and CFEs were used to record DA release in the grafted areas (Fig. 4*A*, *Right*). Local application of 70-mM K^+ induced repeatable DA signals represented by the amperometric current I_{amp}, both in intact and pNSC–DAn-grafted striatal slices (Fig. S6). In contrast, the depolarization-evoked DA overflow was diminished in striatal

Fig. 3. Microdialysis-based HPLC analysis of DA and its metabolites from pNSC–DAn-grafted striatum evoked by local application of 70-mM K^+ in vivo. (*A*) Representative HPLC chromatograms after 70-mM K^+ stimulation in the striatum of intact control (Ctrl), PD–PBS, and PD–DAn rats in vivo. DA and its metabolites DOPAC and HVA were detected. Expanded DA signals are shown in the *Right* panel. (*B*) Statistical analysis showing that the levels of DA, DOPAC, and HVA were reduced in PD–PBS rats, and the DA level was rescued in PD–DAn rats (Student *t* test; ***$P < 0.001$, **$P < 0.01$, *$P < 0.05$; $n = 6$ for Ctrl; $n = 5$ for PD–PBS; $n = 5$ for PD–DAn). Left axis, [DA]; right axis, rescue by transplantation.

Fig. 4. Amperometric recording (I_{amp}) of depolarization-induced DA overflow in pNSC–DAn-grafted striatal slices. (*A*) Micrographs showing grafted pNSC–DAn and the setup for the recording of evoked I_{amp} signals in a striatal slice from a PD–DAn rat. (*Left*) Representative fluorescence micrograph showing the grafted pNSC–DAns (dashed circle). (Scale bar, 200 μm.) (*Inset*) pNSC–DAn at higher resolution. (*Right*) Identification of grafted pNSC–DAns (dashed circle) under a differential interference contrast (DIC) microscope. (Scale bar, 200 μm.) CFE and puffer pipette (for depolarization) as indicated. (*B*) pNSC–DAn-rescued I_{amp} signals in PD rats. Representative I_{amp} signal responses to a 10-s stimulus of 70-mM K$^+$ in intact control (Ctrl), PD–PBS, and PD–DAn striatal slices. (*C*) Rescued I_{amp} signals were limited in or near pNSC–DAn graft sites ("1"), but did not appear distant from the grafts ("2"). The cartoon depicts the recording sites in the PD–DAn striatal slice. (*D*) Statistics showing differences of I_{amp} signals in intact control ($n = 13$ slices from 5 rats), PD–PBS ($n = 13$ slices from 4 rats), and PD–DAn ($n = 7$ slices from 6 rats) rats (Student t test; ***$P < 0.001$, **$P < 0.01$). Left axis, I_{amp}; right axis, rescue by transplantation. (*E*) Statistics showing I_{amp} differences between 1 and 2 sites (Student t test; **$P < 0.01$; $n = 7$ slices from 6 rats). Left axis, I_{amp}.

recording CFE (Fig. 5*A*). Perfusion of high K$^+$ for 5 s evoked a repeatable DA release in the intact dorsal striatum (Fig. 5*A* and Fig. S8). The evoked DA overflow was diminished in the striatum on the lesioned side of PD–PBS rats; however, this was partially but significantly rescued in the cell-engrafted striatum in PD–DAn rats (Fig. 5 *B* and *C*). Compared with the intact side, little DA release remained on the lesioned side of PD–PBS rats (Fig. 5*C*) (intact side, 879.0 ± 181.6 pA; PD–PBS side, 24.4 ± 10.9 pA; $P < 0.01$), whereas the latter recovered to 152.4 ± 18.1 pA (Fig. 5*C*; $P < 0.001$) in PD–DAn rats, with kinetics similar to that in the intact side (Fig. 5*D*). Because CFEs record the DA overflow at the millisecond scale, the kinetics of DA release (I_{amp} rising phase) during stimulation and the immediately subsequent DA reuptake (I_{amp} decay phase) can be clearly separated. The decay

time constant (τ_{decay}) was similar in the cell-grafted and intact sides of the striatum (Fig. 5*D*), suggesting that the DA reuptake in the pNSC–DAn-grafted striatum was rescued as well. In addition, although DA release was smaller in the grafted striatum than in the control side, the rise times and half-height durations (HHDs) were similar (Fig. 5*D*). Together, the increased DA overflow signals in the grafted striatum were mainly due to DA release from grafted pNSC–DAns. In summary, by combining the two in vivo DA detection methods of microdialysis-based HPLC (for DA identification) and CFE amperometry (for real-time DA recording), we demonstrated that the transplanted ESC-derived DA-like neurons directly release DA in the PD striatum in vivo and thus reduce PD behaviors in rats (Fig. 6).

Discussion

One major finding in the present work was the rescue of DA release by grafted pNSC–DAns in the striatum in vivo. Cell-replacement therapy for PD using fetal midbrain cells has been attempted (2, 41–43), but its application raises ethical issues. To overcome the main problem of cell sources for transplantation, extensive efforts have been made to generate DAns from renewable pluripotent stem cells

Fig. 5. Amperometric recording of depolarization-induced DA overflow in pNSC–DAn-grafted striatum in vivo. (*A*) Representative striatal I_{amp} signals in response to a 5-s local application of 70-mM K$^+$ in intact control rats in vivo (*Left*). The I_{amp} signal-recording system is shown in the *Right* panel. A pcCFE consisting of a puffer tube coupled to a CFE with glue (blue; see *Materials and Methods*) was inserted into the grafted striatum (green). (*B*) HHD, decay time (τ_{decay}), and rise time (T_{rise}) were similar on the grafted and intact control sides in PD–DAn rats. (*C*) pNSC–DAn rescued I_{amp} signals in PD rats. Representative I_{amp} in response to a 5-s stimulus of 70 mM K$^+$ in intact control (Ctrl), PD–PBS, and PD–DAn rats in vivo. (*D*) Statistics showing significant differences between I_{amp} signals in intact control ($n = 6$), PD–PBS ($n = 4$), and PD–DAn ($n = 5$) rats in vivo (Student t test; ***$P < 0.001$, **$P < 0.01$). Left axis, I_{amp}; right axis, rescue by transplantation.

NEUROSCIENCE

Fig. 6. Summary schema of pNSC–DAn transplantation and recording of DA release with CFEs in striatum in vivo. (*A*) Experimental procedure for striatal transplantation of pNSC–DAn and major output. (*B*) Exogenous pNSC–DAns (green) were implanted into the damaged striatum, whereas the striatum on the other side (gray) was left intact. A laboratory-made probe (pcCFE) with both a recording CFE and drug-delivery tube [fixed together by glue (blue)] (see *Materials and Methods* for details) was used for in vivo recording. (*C*) Comparison of experimental probes used for DA detection in the brain with microdialysis HPLC or amperometry (CFE). The higher temporal and spatial resolution of amperometry makes it possible for us to precisely record the kinetics and location of DA release. (*D*) Amperometric detection of DA release from grafted pNSC–DAns. When sufficient potential (780 mV) is applied to the electrode, DA is oxidized to DA-o-quinone, donating two electrons per DA molecule that are detected as amperometric current (I_{amp}), which can be calibrated with DA concentration [DA]. (*Inset*) Typical trace recorded by a CFE with perfusion of 70-mM K^+.

(11, 17, 44, 45). Since 2011, several groups including ours have developed a rapid and highly efficient method to differentiate human ESCs into renewable pNSCs, which subsequently produce massive numbers of DA-like neurons for PD treatment (12, 18, 19). Importantly, striatal transplantation of pNSC–DAns significantly relieved the asymmetric rotation in a unilaterally damaged PD rat model (present work and see also refs. 12, 19). In the present work, we demonstrated that pNSC–DAn transplantation rescued DA release in the PD striatum, as determined by both microdialysis-based HPLC (for unequivocal DA verification) and CFE amperometry (for high spatiotemporal resolution) recordings in vivo.

The second major finding was determination of the cellular site of DA release in pNSC–DAn-transplanted striatal brain slices. Previous studies have shown that grafted cells can survive and reduce PD-like behaviors (6, 8–10, 13, 14). In addition, DA release can be rescued in vivo by both mouse (33) and human

(present work) ESC-derived cells in the grafted rat striatum. However, the critical question of whether the grafted cells release DA in vivo remained unanswered because the spatial (200 μm) and temporal (500 s) resolution of microdialysis-based HPLC was too low to distinguish grafted cells from residual cells within the implanted striatum. In contrast, DA recording by CFE amperometry has much higher spatial resolution (probe diameter, 7 μm versus 200 μm) temporal resolution (sample rate, 1 ms versus 10 min) (Fig. 6*C*), making it possible to precisely record the location and kinetics of microregional DA release in striatal brain slices under a microscope. Strikingly, the restored DA release was limited to the grafted regions (Fig. 4). Considering that the differentiated pNSCs were able to secrete DA in vitro and that the diminished TH staining in the lesioned striatum was rescued by the engraftment of pNSC–DAn and that most of the TH-positive cell bodies and neurites were also GFP-positive (Fig. 2 *A–C* and Fig. S4), the increased DA level in the striatum is most likely directly released from the grafted pNSC–DAns.

With high-resolution CFE recordings, another finding was that pNSC–DAn rescued DA reuptake in slices from the grafted striatum and in vivo. Here, the kinetics of evoked DA release and reuptake in the grafted PD striatum were determined by the amperometric current with high temporal resolution, in which the rise time represents DA release and the decay time indicates DA reuptake (34, 46–48). Interestingly, the depolarization-induced DA dynamics in the PD-grafted striatum were similar to those in the intact side, as evidenced by comparable rise times, HHDs, and decay times in the pNSC–DAn-grafted and intact sides of the striatum (Fig. 5). Thus, the DA release-coupled clearance was rescued by the grafted pNSC–DAn as well.

Altogether, human ESC-derived pNSC–DA cells can be functionally integrated into the striatum. As summarized in Fig. 6, the present study demonstrated that the rescued DA release and reuptake was most likely from grafted cells. Because human ESC-derived pNSCs, and probably also induced pluripotent stem cells from patients, have high efficacy for producing virtually infinite numbers of transplantable DAns, our work provides an in vivo mechanism for potential application of human ESCs in the treatment of PD.

Materials and Methods

Methods are described in detail in *SI Materials and Methods*. All animal procedures were approved by and performed according to the guidelines of the Peking University Animal Use and Care Committee and the Association for Assessment and Accreditation of Laboratory Animal Care.

Cell Culture and Differentiation of DAns. pNSCs were induced from human ESCs as previously described (18).

PD Model, Behavioral Testing, and Cell Transplantation. Adult male Sprague–Dawley rats (~200 g) were microinjected with 6-OHDA into MFB to produce the PD model. The differentiated pNSC–DAns were microinjected into the ipsilateral striatum of the leisoned side of the PD rat, with PBS as the control. The rats were immunosuppressed by daily injection of cyclosporine A from 2 d before transplantation. Apomorphine-induced rotations were monitored every 4 wk after transplantation.

HPLC Detection of DA Release in Vitro and in Vivo. Microdialysis-based HPLC detection of the striatal DA and its metabolites were performed as described previously (32), with slight modifications. Cultured pNSC–DAns were incubated in the 3-mM K^+-containing solution for 5 min, followed by 50 mM of the K^+-containing solution for another 5 min, and the bath solution was collected for HPLC analysis.

Amperometric Recording in Vivo and in Striatal Slices. Electrochemical amperometric current (I_{amp}) was recorded in brain slices and in vivo using CFEs, as previously described (34, 37). DA release was recorded as I_{amp} (oxidization amperometric current) by a CFE (Φ7 μm) with a 200-μm sensor tip held at 780 mV. For in vivo recording of DA release in striatum, the anesthetized rat was stimulated and recorded by a laboratory-made puffer-coupled CFE (pcCFE), which is consisted of a combined CFE and delivery tube (Fig. 6*B*). The pcCFE was placed in the striatum, and DA release was evoked by perfusion of 70 mM K^+ through the drug-delivery tube. DA recording of striatal slices was performed as previously described (49). DA overflow was evoked by perfusion with 70 mM K^+ for 10 s and recorded by CFE.

Immunohistochemistry. Immunohistochemistry was performed as previously described (49, 50), with slight modifications. Briefly, rats were anesthetized and prefixed with 4% (wt/vol) paraformaldehyde through transcardial perfusion. The brain was postfixed, dehydrated, and sectioned at 50 μm on a cryostat. Cultured cells were fixed with 4% (wt/vol) paraformaldehyde in PBS. The fixed samples were permeabilized, blocked, and then incubated with primary antibodies, followed by secondary antibodies. Samples were observed using a Zeiss 710 inverted confocal microscope.

Statistical Analysis. At least three independent experiments were performed for each type of assay. Comparisons were made with the two-tailed unpaired Student t test or one-way ANOVA as indicated. All tests were performed using the Statistical Package for the Social Sciences version 13.0, and significant differences were accepted at $P < 0.05$.

1. Olanow CW, Tatton WG (1999) Etiology and pathogenesis of Parkinson's disease. *Annu Rev Neurosci* 22:123–144.
2. Barker RA, Barrett J, Mason SL, Björklund A (2013) Fetal dopaminergic transplantation trials and the future of neural grafting in Parkinson's disease. *Lancet Neurol* 12(1):84–91.
3. Lindvall O, et al. (1990) Grafts of fetal dopamine neurons survive and improve motor function in Parkinson's disease. *Science* 247(4942):574–577.
4. Piccini P, et al. (1999) Dopamine release from nigral transplants visualized in vivo in a Parkinson's patient. *Nat Neurosci* 2(12):1137–1140.
5. Freed CR, et al. (1992) Survival of implanted fetal dopamine cells and neurologic improvement 12 to 46 months after transplantation for Parkinson's disease. *N Engl J Med* 327(22):1549–1555.
6. Kordower JH, et al. (1995) Neuropathological evidence of graft survival and striatal reinnervation after the transplantation of fetal mesencephalic tissue in a patient with Parkinson's disease. *N Engl J Med* 332(17):1118–1124.
7. Widner H, et al. (1992) Bilateral fetal mesencephalic grafting in two patients with parkinsonism induced by 1-methyl-4-phenyl-1,2,3,6-tetrahydropyridine (MPTP). *N Engl J Med* 327(22):1556–1563.
8. Bjorklund LM, et al. (2002) Embryonic stem cells develop into functional dopaminergic neurons after transplantation in a Parkinson rat model. *Proc Natl Acad Sci USA* 99(4):2344–2349.
9. Hargus G, et al. (2010) Differentiated Parkinson patient-derived induced pluripotent stem cells grow in the adult rodent brain and reduce motor asymmetry in Parkinsonian rats. *Proc Natl Acad Sci USA* 107(36):15921–15926.
10. Kim J, et al. (2011) Functional integration of dopaminergic neurons directly converted from mouse fibroblasts. *Cell Stem Cell* 9(5):413–419.
11. Kim JH, et al. (2002) Dopamine neurons derived from embryonic stem cells function in an animal model of Parkinson's disease. *Nature* 418(6893):50–56.
12. Kriks S, et al. (2011) Dopamine neurons derived from human ES cells efficiently engraft in animal models of Parkinson's disease. *Nature* 480(7378):547–551.
13. Roy NS, et al. (2006) Functional engraftment of human ES cell-derived dopaminergic neurons enriched by coculture with telomerase-immortalized midbrain astrocytes. *Nat Med* 12(11):1259–1268.
14. Studer L, Tabar V, McKay RD (1998) Transplantation of expanded mesencephalic precursors leads to recovery in parkinsonian rats. *Nat Neurosci* 1(4):290–295.
15. Yang D, Zhang ZJ, Oldenburg M, Ayala M, Zhang SC (2008) Human embryonic stem cell-derived dopaminergic neurons reverse functional deficit in parkinsonian rats. *Stem Cells* 26(1):55–63.
16. Lee SH, Lumelsky N, Studer L, Auerbach JM, McKay RD (2000) Efficient generation of midbrain and hindbrain neurons from mouse embryonic stem cells. *Nat Biotechnol* 18(6):675–679.
17. Perrier AL, et al. (2004) Derivation of midbrain dopamine neurons from human embryonic stem cells. *Proc Natl Acad Sci USA* 101(34):12543–12548.
18. Li W, et al. (2011) Rapid induction and long-term self-renewal of primitive neural precursors from human embryonic stem cells by small molecule inhibitors. *Proc Natl Acad Sci USA* 108(20):8299–8304.
19. Kirkeby A, et al. (2012) Generation of regionally specified neural progenitors and functional neurons from human embryonic stem cells under defined conditions. *Cell Reports* 1(6):703–714.
20. Cho MS, et al. (2008) Highly efficient and large-scale generation of functional dopamine neurons from human embryonic stem cells. *Proc Natl Acad Sci USA* 105(9):3392–3397.
21. Kawasaki H, et al. (2000) Induction of midbrain dopaminergic neurons from ES cells by stromal cell-derived inducing activity. *Neuron* 28(1):31–40.
22. Takagi Y, et al. (2005) Dopaminergic neurons generated from monkey embryonic stem cells function in a Parkinson primate model. *J Clin Invest* 115(1):102–109.
23. Zeng X, et al. (2004) Dopaminergic differentiation of human embryonic stem cells. *Stem Cells* 22(6):925–940.
24. Gobert A, Billiras R, Cistarelli L, Millan MJ (2004) Quantification and pharmacological characterization of dialysate levels of noradrenaline in the striatum of freely-moving rats: Release from adrenergic terminals and modulation by alpha2-autoreceptors. *J Neurosci Methods* 140(1-2):141–152.
25. Sara SJ (2009) The locus coeruleus and noradrenergic modulation of cognition. *Nat Rev Neurosci* 10(3):211–223.
26. Hoffman AF, Lupica CR, Gerhardt GA (1998) Dopamine transporter activity in the substantia nigra and striatum assessed by high-speed chronoamperometric recordings in brain slices. *J Pharmacol Exp Ther* 287(2):487–496.
27. Gerhardt GA, Oke AF, Nagy G, Moghaddam B, Adams RN (1984) Nafion-coated electrodes with high selectivity for CNS electrochemistry. *Brain Res* 290(2):390–395.
28. Kehr J (1999) *Monitoring Chemistry of Brain Microenvironment: Biosensors, Microdialysis and Related Techniques. Modern Techniques in Neuroscience Research*, eds Windhorst U, Johansson H (Springer, Berlin), pp 1149–1198.
29. Ourednik J, Ourednik V, Lynch WP, Schachner M, Snyder EY (2002) Neural stem cells display an inherent mechanism for rescuing dysfunctional neurons. *Nat Biotechnol* 20(11):1103–1110.
30. Redmond DE, Jr, et al. (2007) Behavioral improvement in a primate Parkinson's model is associated with multiple homeostatic effects of human neural stem cells. *Proc Natl Acad Sci USA* 104(29):12175–12180.
31. Bouchez G, et al. (2008) Partial recovery of dopaminergic pathway after graft of adult mesenchymal stem cells in a rat model of Parkinson's disease. *Neurochem Int* 52(7):1332–1342.
32. Liu K, Steketee JD (2011) Repeated exposure to cocaine alters medial prefrontal cortex dopamine D_2-like receptor modulation of glutamate and dopamine neurotransmission within the mesocorticolimbic system. *J Neurochem* 119(2):332–341.
33. Rodríguez-Gómez JA, et al. (2007) Persistent dopamine functions of neurons derived from embryonic stem cells in a rodent model of Parkinson disease. *Stem Cells* 25(4):918–928.
34. Wang SR, et al. (2011) Role of vesicle pools in action potential pattern-dependent dopamine overflow in rat striatum in vivo. *J Neurochem* 119(2):342–353.
35. Wightman RM (2006) Detection technologies. Probing cellular chemistry in biological systems with microelectrodes. *Science* 311(5767):1570–1574.
36. Anzalone A, et al. (2012) Dual control of dopamine synthesis and release by presynaptic and postsynaptic dopamine D2 receptors. *J Neurosci* 32(26):9023–9034.
37. Huang HP, et al. (2007) Long latency of evoked quantal transmitter release from somata of locus coeruleus neurons in rat pontine slices. *Proc Natl Acad Sci USA* 104(4):1401–1406.
38. Wightman RM, et al. (1991) Temporally resolved catecholamine spikes correspond to single vesicle release from individual chromaffin cells. *Proc Natl Acad Sci USA* 88(23):10754–10758.
39. Chen XK, et al. (2005) Activation of GPCRs modulates quantal size in chromaffin cells through G(betagamma) and PKC. *Nat Neurosci* 8(9):1160–1168.
40. Zhou Z, Misler S (1995) Action potential-induced quantal secretion of catecholamines from rat adrenal chromaffin cells. *J Biol Chem* 270(8):3498–3505.
41. Kordower JH, Chu Y, Hauser RA, Freeman TB, Olanow CW (2008) Lewy body-like pathology in long-term embryonic nigral transplants in Parkinson's disease. *Nat Med* 14(5):504–506.
42. Lindvall O, Kokaia Z, Martinez-Serrano A (2004) Stem cell therapy for human neurodegenerative disorders—How to make it work. *Nat Med* 10(Suppl):S42–S50.
43. Dunnett SB, Björklund A, Lindvall O (2001) Cell therapy in Parkinson's disease—Stop or go? *Nat Rev Neurosci* 2(5):365–369.
44. Chung S, et al. (2011) ES cell-derived renewable and functional midbrain dopaminergic progenitors. *Proc Natl Acad Sci USA* 108(23):9703–9708.
45. Ganat YM, et al. (2012) Identification of embryonic stem cell-derived midbrain dopaminergic neurons for engraftment. *J Clin Invest* 122(8):2928–2939.
46. Mundorf ML, Joseph JD, Austin CM, Caron MG, Wightman RM (2001) Catecholamine release and uptake in the mouse prefrontal cortex. *J Neurochem* 79(1):130–142.
47. Schmitz Y, Schmauss C, Sulzer D (2002) Altered dopamine release and uptake kinetics in mice lacking D2 receptors. *J Neurosci* 22(18):8002–8009.
48. Wu Q, et al. (2002) Concurrent autoreceptor-mediated control of dopamine release and uptake during neurotransmission: An in vivo voltammetric study. *J Neurosci* 22(14):6272–6281.
49. Wang L, et al. (2014) Modulation of dopamine release in the striatum by physiologically relevant levels of nicotine. *Nat Commun* 5:3925.
50. Liu T, et al. (2011) Calcium triggers exocytosis from two types of organelles in a single astrocyte. *J Neurosci* 31(29):10593–10601.

NEUROSCIENCE